Harmonic Green's functions of a semi-infinite plate with clamped or free edges

R. Gunda, S. M. Vijayakar, R. Singh,[a] and J. E. Farstad
Department of Mechanical Engineering, Acoustics and Dynamics Laboratory, The Ohio State University, 206 W. 18th Avenue, Columbus, Ohio 43210-1107

(Received 4 August 1997; accepted for publication 14 October 1997)

Harmonic Green's functions for a thin semi-infinite plate with clamped or free edges are developed starting from either simply supported or roller supported solutions and applying corrections to account for boundary excitation. This is achieved by connecting the solutions in terms of polar coordinates with the solutions in Cartesian coordinates. The formal solutions in the form of improper wave-number integrals are numerically evaluated using adaptive Clenshaw–Curtis integration. Alternate solutions obtained for each boundary condition compare well. Only harmonic point loads are considered in this article but the methodology may be extended to moment excitation and distributed loads. The methodology developed here will form the basis for advancing the ray tracing technique for vibration analysis of finite plates. © *1998 Acoustical Society of America.* [S0001-4966(98)02302-9]

PACS numbers: 43.40.Dx, 43.40.At [CBB]

INTRODUCTION

The Green's functions for the harmonic response of semi-infinite plates serve as the basis for a ray tracing method used to construct solutions in finite domains and for boundary element models. The ray tracing technique has already been implemented successfully to predict harmonic responses in beams and rectangular plates with simply supported and roller supported boundary conditions.[1] New solutions needed for clamped and free edges are developed in this article.

A similar problem of interest to seismologists is the propagation of tremors over the surface of an elastic half-space due to harmonic line sources on the surface[2] or buried line sources radiating cylindrical[3] or conical[4] pulses. The main focus in elastic half-space problems is the wave propagation on the free surface. Other investigators have examined the acoustic radiation Green's functions for fluid-filled elastic plates governing the production of aerodynamic sound by sources near the edges of a semi-infinite plate[5] or an infinite plate with discontinuities.[6]

To the best of our knowledge, two studies have specifically addressed the Green's functions for semi-infinite plates. Ortner[7] uses the semi-infinite clamped beam solution to obtain the dynamic Green's function for a clamped semi-infinite plate with a special orthrotropic property. He uses Laplace–Fourier transform techniques to derive the dynamic Green's function in the form of a double integral but it was not evaluated numerically. Static Green's function for a clamped semi-infinite plate on an elastic foundation was obtained by adding clamping terms to the simply supported solution. Similarly Kerr[8] derives the static Green's functions for a clamped semi-infinite plate on a Winkler foundation by formulating an integral equation for an unknown distributed load on the boundary line and by adding clamping terms to the roller supported solution.

I. PROBLEM FORMULATION

A. Governing equations

The equation governing the transverse motion $w(\mathbf{r},t)$ of an isotropic homogeneous plate of constant thickness (h) is given by classical thin plate theory[9] as

$$D\nabla^4 w(\mathbf{r},t)+\rho h\frac{\partial^2}{\partial t^2}w(\mathbf{r},t)=p(\mathbf{r},t)\forall\,\mathbf{r}\in\Omega, \tag{1}$$

where $D=Eh^3/12(1-\nu^2)$ is the flexural rigidity of the plate, E is the Young's modulus, ν is the Poisson's ratio, ∇^4 is the biharmonic operator, ρ is the mass density, $p(\mathbf{r},t)$ is the normal force per unit area, $\mathbf{r}$ the position vector, and t is the time. For harmonic excitation at a constant circular frequency ω, $p(\mathbf{r},t)=\hat{p}(\mathbf{r})\exp(-i\omega t)$, the response will be $w(\mathbf{r},t)=\hat{w}(\mathbf{r})\exp(-i\omega t)$, allowing us to suppress the time dependence from Eq. (1) and carry out the analysis in the frequency domain. Thus Eq. (1) can be rewritten as

$$(\nabla^4-k^4)\hat{w}(\mathbf{r})=\frac{\hat{p}(\mathbf{r})}{D};\quad k^4=\frac{\rho h\omega^2}{D}, \tag{2}$$

where k is the bending wave number. Structural damping behavior is incorporated in the formulation by substituting $D(1-i\eta)$ for D in Eq. (2), η being the structural loss factor. The negative sign in $D(1-i\eta)$ is chosen to yield behavior consistent with equivalent viscous damping for the $\exp(-i\omega t)$ time dependence.

B. Boundary conditions

At a regular point (not a corner) on a continuous boundary $\partial\Omega$, the bending moment $M_n(w)$, twisting moment $M_t(w)$, shear force $Q_n(w)$, and Kelvin–Kirchhoff edge reaction $V_n(w)$ are given by the following expressions:[10]

[a]Electronic mail: singh.3@osu.edu

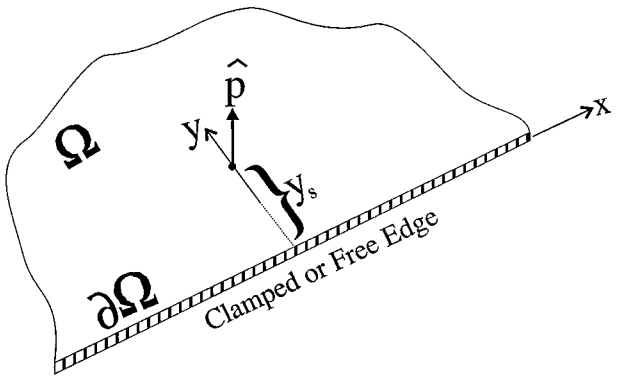

FIG. 1. The problem geometry, loading, and boundary conditions.

$$M_n(w)=\frac{D}{2}\left\{-(1+\nu)\nabla^2 w+(1-\nu)\left[\left(\frac{\partial^2 w}{\partial y^2}-\frac{\partial^2 w}{\partial x^2}\right)\times\cos 2\alpha-2\frac{\partial^2 w}{\partial x\partial y}\sin 2\alpha\right]\right\}\mathbf{e_t}, \tag{3}$$

$$M_t(w)=\frac{D(1-\nu)}{2}\left[\left(\frac{\partial^2 w}{\partial y^2}-\frac{\partial^2 w}{\partial x^2}\right)\sin 2\alpha+2\frac{\partial^2 w}{\partial x\partial y}\cos 2\alpha\right]\mathbf{e_n}, \tag{4}$$

$$Q_n(w)=-D\frac{\partial}{\partial n}(\nabla^2 w)\mathbf{e_z}, \tag{5}$$

$$V_n(w)=\left\{-D\frac{\partial}{\partial n}(\nabla^2 w)-\frac{\partial M_t}{\partial s}\right\}\mathbf{e_z}, \tag{6}$$

where $\cos\alpha=\mathbf{n}\cdot\mathbf{e_x}$ and $\sin\alpha=\mathbf{n}\cdot\mathbf{e_y}$ are the direction cosines of the outward normal $\mathbf{n}$, s is the tangential coordinate considered positive in the counterclockwise direction, $\mathbf{e_x},\mathbf{e_y},\mathbf{e_z}$ are the unit vectors in the coordinate directions, and $\mathbf{e_n},\mathbf{e_t}$ are the unit vectors along $\mathbf{n}$, $\partial\Omega$, respectively. The four classical boundary conditions are simple supports, roller supports, clamped, and free edges, which satisfy the following relations on $\partial\Omega$:

$$\begin{aligned}&\text{simple supports (S):}\quad w=0,\quad M_n(w)=0,\\&\text{roller supports (R):}\quad \partial w/\partial n=0,\quad V_n(w)=0,\\&\text{clamped edge (C):}\quad w=0,\quad \partial w/\partial n=0,\\&\text{free edge (F):}\quad M_n(w)=0,\quad V_n(w)=0.\end{aligned} \tag{7}$$

C. Statement of the problem

Figure 1 illustrates the plate geometry along with the excitation and boundary conditions. Without loss of generality, the semi-infinite plate is assumed to be oriented such that its edge coincides with the x axis of the coordinate system. The plate domain Ω is given by $\Omega=\{(x,y)/y\geqslant 0\}$. The plate is excited by a unit harmonic force concentrated at $\mathbf{r_s}=(0,y_s)$. Hence $\hat{p}(\mathbf{r})=\delta(\mathbf{r}-\mathbf{r_s})$, δ being the Dirac's delta function. On the plate edge $(y=0)$, one of the four classical boundary conditions described by Eq. (7) is applied. In addition, the Sommerfeld radiation condition must be satisfied as the observation point approaches infinity in the y direction (as $y\to\infty$). We seek to derive analytical harmonic Green's functions of Eq. (2) in Ω for the excitation and boundary conditions as described above.

D. Infinite plate solution

The Green's function for an infinite plate $G_\infty(\mathbf{r}|\mathbf{r_s};k)$ represents the transverse deflection $\hat{w}(\mathbf{r})$ due to a unit concentrated harmonic load $\hat{p}(\mathbf{r})=\delta(\mathbf{r}-\mathbf{r_s})$ at $\mathbf{r_s}$:

$$G_\infty(\mathbf{r}|\mathbf{r_s};k)=C[H_0^1(kr)-H_0^1(ikr)],\quad C=\frac{i}{8k^2D}, \tag{8}$$

where $r=|\mathbf{r}-\mathbf{r_s}|$ is the distance of the observation point from the source location and H_0^1 is the zero order Hankel function of the first kind. The fundamental solution given by Eq. (8) satisfies the Sommerfeld radiation condition at infinity which requires the source to yield only outgoing waves. This is evident from the asymptotic expansion of the Hankel functions for large argument.[11]

In this paper, the Green's functions for the semi-infinite plate are obtained by adding correction terms to the infinite plate fundamental solution $G_\infty(\mathbf{r}|\mathbf{r_s};k)$ to account for the boundary conditions. The representation for $G_\infty(\mathbf{r}|\mathbf{r_s};k)$ given by Eq. (8) contains both the arguments x,y under the radical as $\{(x-x_s)^2+(y-y_s)^2\}^{1/2}$ making it inconvenient for applying boundary conditions along the edge $y=0$. Hence it is advantageous to transform $G_\infty(\mathbf{r}|\mathbf{r_s};k)$ by decomposing the Hankel functions into their Cartesian components. This is accomplished by comparing two representations of the solution U to the two-dimensional Helmholtz equation (wave equation in frequency domain) excited by a unit harmonic point source at the origin:

$$\nabla^2 U+k^2 U=\delta(\mathbf{r}). \tag{9}$$

Equation (9) in cylindrical polar coordinates is

$$\frac{\partial^2 U}{\partial r^2}+\frac{1}{r}\frac{\partial U}{\partial r}+k^2 U=\frac{\delta(r)}{2\pi r}. \tag{10}$$

The solution U should in addition satisfy the Sommerfeld radiation condition. The homogeneous form of Eq. (10) is the Bessel's differential equation of order zero. The solution U is obtained by solving Eq. (10) in its homogeneous form and adjusting the coefficients to account for the source at the origin. Therefore $U(\mathbf{r})=AH_0^1(kr)$. Integrating Eq. (10) over a small circle around the origin and taking the limit as the radius of the circle approaches zero yields $A=1/4i$. Therefore

$$U(\mathbf{r})=\frac{1}{4i}H_0^1(kr). \tag{11}$$

Equation (9) in Cartesian coordinates is

$$\frac{\partial^2 U}{\partial x^2}+\frac{\partial^2 U}{\partial y^2}+k^2 U=\delta(x)\,\delta(y). \tag{12}$$

Applying the spatial Fourier transform in the x direction to Eq. (12) yields

$$-k_x^2\overline{U}(k_x,y)+\frac{\partial^2\overline{U}(k_x,y)}{\partial y^2}+k^2\overline{U}(k_x,y)=\frac{1}{\sqrt{2\pi}}\delta(y). \tag{13}$$

Let $k_y^2=k^2-k_x^2$. Equation (13) simplifies to

$$\frac{\partial^2\overline{U}(k_x,y)}{\partial y^2}+k_y^2\overline{U}(k_x,y)=\frac{1}{\sqrt{2\pi}}\delta(y). \tag{14}$$

Equation (14) is the one-dimensional wave equation in frequency domain whose solution[12] is

$$\overline{U}(k_x,y)=\frac{1}{\sqrt{2\pi}}\frac{1}{2ik_y}e^{ik_y|y|}\quad \mathrm{Im}(k_y),\ \ \mathrm{Re}(k_y)\geqslant 0. \tag{15}$$

Taking the inverse spatial Fourier transform of Eq. (15) in the x direction yields the required solution $U(\mathbf{r})$:

$$U(\mathbf{r})=\frac{1}{4\pi i}\int_{-\infty}^{\infty}\frac{e^{ik_xx}e^{ik_y|y|}}{k_y}dk_x$$
$$=\frac{1}{2\pi i}\int_0^{\infty}\frac{\cos k_xx e^{ik_y|y|}}{k_y}dk_x. \tag{16}$$

Comparing Eq. (11) with Eq. (16), we get the desired Cartesian decomposition of the zero order Hankel function of the first kind, and a representation of the fundamental solution suitable for applying boundary conditions along the straight edge ($y=0$) in terms of a wave-number integral as follows:

$$H_0^1(kr)=\frac{1}{\pi}\int_{-\infty}^{\infty}\frac{\exp(ik_xx)e^{ik_y|y|}}{k_y}dk_x,$$
$$\mathrm{Im}(k_y),\ \ \mathrm{Im}(k)\geqslant 0, \tag{17}$$

$$G_\infty(\mathbf{r}|\mathbf{r_s};k)=\frac{C}{\pi}\int_{-\infty}^{\infty}e^{ik_x(x-x_s)}\left[\frac{e^{i\sqrt{k^2-k_x^2}|y-y_s|}}{\sqrt{k^2-k_x^2}}+i\frac{e^{-\sqrt{k^2+k_x^2}|y-y_s|}}{\sqrt{k^2+k_x^2}}\right]dk_x. \tag{18}$$

II. FORMULATION FOR SEMI-INFINITE PLATE

A. Simply supported and roller supported edges

The solution for a semi-infinite plate with a simply supported edge excited by a point load at $\mathbf{r_s}=(0,y_s)$ is given by the method of images[1] as

$$G_s(\mathbf{r}|\mathbf{r_s};k)=G_\infty(\mathbf{r}|\mathbf{r_s};k)-G_\infty(\mathbf{r}|\mathbf{r_i};k), \tag{19}$$

where $\mathbf{r_i}=(0,-y_s)$ is the location of image of $\mathbf{r_s}$ in the plate edge. This solution satisfies the conditions of vanishing transverse displacement $\hat{w}$ and the bending moment $M_n(\hat{w})$ on the plate edge. The normal slope $\partial\hat{w}/\partial n$ and the edge reaction $V_n(\hat{w})$ along the edge ($y=0$) are given by

$$\frac{\partial\hat{w}}{\partial n}=-\frac{\partial\hat{w}}{\partial y}=\frac{2Ci}{\pi}\int_{-\infty}^{\infty}\exp(ik_xx)[e^{i\sqrt{k^2-k_x^2}y_s}-e^{-\sqrt{k^2+k_x^2}y_s}]dk_x, \tag{20}$$

$$V_n(\hat{w})=\frac{2CDi}{\pi}\int_{-\infty}^{\infty}\exp(ik_xx)\times[\{k^2+(1-\nu)k_x^2\}e^{i\sqrt{k^2-k_x^2}y_s}+\{k^2-(1-\nu)k_x^2\}e^{-\sqrt{k^2+k_x^2}y_s}]dk_x. \tag{21}$$

Like the simply supported case, the solution for the roller supported edge is obtained from the method of images as

$$G_r(\mathbf{r}|\mathbf{r_s};k)=G_\infty(\mathbf{r}|\mathbf{r_s};k)+G_\infty(\mathbf{r}|\mathbf{r_i};k). \tag{22}$$

This solution has zero normal slope $\partial\hat{w}/\partial n$ and zero edge reaction $V_n(\hat{w})$ on the plate edge. The transverse deflection $\hat{w}$ and the bending moment $M_n(\hat{w})$ along the edge are given by

$$\hat{w}=\frac{2C}{\pi}\int_{-\infty}^{\infty}\exp(ik_xx)\times\left[\frac{e^{i\sqrt{k^2-k_x^2}y_s}}{\sqrt{k^2-k_x^2}}+i\frac{e^{-\sqrt{k^2+k_x^2}y_s}}{\sqrt{k^2+k_x^2}}\right]dk_x, \tag{23}$$

$$M_n(\hat{w})=\frac{2CD}{\pi}\int_{-\infty}^{\infty}\exp(ik_xx)\times\left[\{k^2-(1-\nu)k_x^2\}\frac{e^{i\sqrt{k^2-k_x^2}y_s}}{\sqrt{k^2-k_x^2}}-i\{k^2+(1-\nu)k_x^2\}\frac{e^{-\sqrt{k^2+k_x^2}y_s}}{\sqrt{k^2+k_x^2}}\right]dk_x. \tag{24}$$

B. Clamped edge via correction to roller supported edge

In this section, the Green's function for a clamped edge is obtained by adding to $G_r(\mathbf{r}|\mathbf{r_s};k)$ given by Eq. (22), terms corresponding to certain waves which travel along the edge and decay or propagate in the plate interior. However, a simpler problem of a semi-infinite plate subjected to the following boundary excitation needs to be solved first: $\hat{w}=W(k_x)\exp(ik_xx)$ on $y=0$ and $\partial\hat{w}/\partial n=0$ on $y=0$. A trial function which satisfies the homogeneous form of governing Eq. (2) is

$$\hat{w}(\mathbf{r})=\exp(ik_xx)[A(k_x)e^{i\sqrt{k^2-k_x^2}y}+B(k_x)e^{-\sqrt{k^2+k_x^2}y}]. \tag{25}$$

The solution given by Eq. (25) is suitable for any type of boundary excitation since it yields bounded responses [waves propagating in the interior (first term if $k_x<k$), and waves traveling along the edge and decaying in the plate interior (second term and first term if $k_x>k$)]. Imposing the boundary conditions leads to the following system of equations for the coefficients $A(k_x)$ and $B(k_x)$:

$$\begin{bmatrix}1 & 1\\ -i\sqrt{k^2-k_x^2} & \sqrt{k^2+k_x^2}\end{bmatrix}\begin{Bmatrix}A(k_x)\\ B(k_x)\end{Bmatrix}=\begin{Bmatrix}W(k_x)\\ 0\end{Bmatrix}. \tag{26}$$

The coefficient matrix in Eq. (26) is never singular. Solving Eq. (26) gives the solution as

$$\hat{w}(\mathbf{r})=\frac{W(k_x)\exp(ik_x x)}{\sqrt{k^2+k_x^2}+i\sqrt{k^2-k_x^2}}\left[\sqrt{k^2+k_x^2}e^{i\sqrt{k^2-k_x^2}y}\right.$$
$$\left.+i\sqrt{k^2-k_x^2}e^{-\sqrt{k^2+k_x^2}y}\right]. \quad (27)$$

In a roller supported plate, the transverse deflection along the edge is given by Eq. (23). The component of wave number k_x is

$$W(k_x)=\frac{2C}{\pi}\left[\frac{e^{i\sqrt{k^2-k_x^2}y_s}}{\sqrt{k^2-k_x^2}}+i\frac{e^{-\sqrt{k^2+k_x^2}y_s}}{\sqrt{k^2+k_x^2}}\right]. \quad (28)$$

The contribution of this edge displacement excitation has to be subtracted from $G_r(\mathbf{r}|\mathbf{r_s};k)$ to realize the clamped boundary condition along $y=0$. Using the principle of superposition, the correction to the roller supported fundamental solution $G_r(\mathbf{r}|\mathbf{r_s};k)$ to obtain the solution to the clamped boundary $G_c(\mathbf{r}|\mathbf{r_s};k)$ is

$$\hat{w}_{cr}(\mathbf{r}|\mathbf{r_s})=\frac{2C}{\pi}\int_{-\infty}^{\infty}\frac{\exp(ik_x x)}{\sqrt{k^2+k_x^2}+i\sqrt{k^2-k_x^2}}\left[\frac{e^{i\sqrt{k^2-k_x^2}y_s}}{\sqrt{k^2-k_x^2}}\right.$$
$$\left.+i\frac{e^{-\sqrt{k^2+k_x^2}y_s}}{\sqrt{k^2+k_x^2}}\right]\left[\sqrt{k^2+k_x^2}e^{i\sqrt{k^2-k_x^2}y}\right.$$
$$\left.+i\sqrt{k^2-k_x^2}e^{-\sqrt{k^2+k_x^2}y}\right]dk_x \quad (29)$$
$$=\frac{2C}{\pi}\int_{-\infty}^{\infty}\frac{\exp(ik_x x)}{\Delta_{cr}}f_{cr}(y)f_{cr}(y_s)dk_x, \quad (30)$$

where Δ_{cr} and $f_{cr}(y)$ are given by

$$\Delta_{cr}=\sqrt{k^2+k_x^2}\sqrt{k^2-k_x^2}\{\sqrt{k^2+k_x^2}+i\sqrt{k^2-k_x^2}\}, \quad (31)$$

$$f_{cr}(y)=\sqrt{k^2+k_x^2}e^{i\sqrt{k^2-k_x^2}y}+i\sqrt{k^2-k_x^2}e^{-\sqrt{k^2+k_x^2}y}. \quad (32)$$

The fundamental solution for the clamped edge $G_c(\mathbf{r}|\mathbf{r_s};k)$ is obtained by subtracting $\hat{w}_{cr}(\mathbf{r}|\mathbf{r_s})$ from $G_r(\mathbf{r}|\mathbf{r_s};k)$:

$$G_c(\mathbf{r}|\mathbf{r_s};k)=G_r(\mathbf{r}|\mathbf{r_s};k)-\hat{w}_{cr}(\mathbf{r}|\mathbf{r_s}). \quad (33)$$

The Green's function $G_c(\mathbf{r}|\mathbf{r_s};k)$ given by Eq. (33) is convenient for calculating the effective shear force per unit length $V_n(\hat{w})$ along the edge $y=0$, since the roller solution $G_r(\mathbf{r}|\mathbf{r_s};k)$ does not contribute and the contribution from correction term $-\hat{w}_{cr}(\mathbf{r}|\mathbf{r_s})$ alone needs to be calculated. Along the edge, $V_n(\hat{w})$ is given by

$$V_n(\hat{w})|_{y=0}=\frac{-1}{2\pi}\int_{-\infty}^{\infty}\frac{\exp(ik_x x)}{\sqrt{k^2+k_x^2}+i\sqrt{k^2-k_x^2}}$$
$$\times\left[\sqrt{k^2+k_x^2}e^{i\sqrt{k^2-k_x^2}y_s}\right.$$
$$\left.+i\sqrt{k^2-k_x^2}e^{-\sqrt{k^2+k_x^2}y_s}\right]dk_x. \quad (34)$$

In the limiting case when y_s approaches zero, from Eq. (34), $V_n(\hat{w})=-1/2\pi\int_{-\infty}^{\infty}\exp(ik_x x)dk_x$ which is nothing but $-\delta(x)$, as it should be.

C. Clamped edge via correction to simply supported edge

In this section, the Green's function for a clamped edge $G_c(\mathbf{r}|\mathbf{r_s};k)$ is obtained by modifying $G_s(\mathbf{r}|\mathbf{r_s};k)$ given by Eq. (19). The simpler problem whose solution is used to construct $G_c(\mathbf{r}|\mathbf{r_s};k)$ is that of a semi-infinite plate with the following boundary excitation: $\hat{w}=0$ on $y=0$ and $\partial\hat{w}/\partial n=W_n(k_x)\exp(ik_x x)$ on $y=0$. Using the trial solution given by Eq. (25) and applying the boundary conditions leads to the following system of equations for the coefficients $A(k_x)$ and $B(k_x)$:

$$\begin{bmatrix}1 & 1\\ -i\sqrt{k^2-k_x^2} & \sqrt{k^2+k_x^2}\end{bmatrix}\begin{Bmatrix}A(k_x)\\ B(k_x)\end{Bmatrix}=\begin{Bmatrix}0\\ W_n(k_x)\end{Bmatrix}. \quad (35)$$

Solving Eq. (35) gives

$$\hat{w}(\mathbf{r})=\frac{W_n(k_x)\exp(ik_x x)}{\sqrt{k^2+k_x^2}+i\sqrt{k^2-k_x^2}}\left[-e^{i\sqrt{k^2-k_x^2}y}+e^{-\sqrt{k^2+k_x^2}y}\right]. \quad (36)$$

In a simply supported plate, the component of wave number k_x of the normal slope along the edge is given by Eq. (20) as

$$W_n(k_x)=\frac{2Ci}{\pi}\left[e^{i\sqrt{k^2-k_x^2}y_s}-e^{-\sqrt{k^2+k_x^2}y_s}\right]. \quad (37)$$

The contribution of this slope excitation is subtracted from $G_s(\mathbf{r}|\mathbf{r_s};k)$ to realize the clamped boundary condition along $y=0$. From superposition, the correction to the simply supported fundamental solution $G_s(\mathbf{r}|\mathbf{r_s};k)$ to obtain the solution to the clamped boundary $G_c(\mathbf{r}|\mathbf{r_s};k)$ is

$$\hat{w}_{cs}(\mathbf{r}|\mathbf{r_s})=\frac{2Ci}{\pi}\int_{-\infty}^{\infty}\frac{\exp(ik_x x)}{\sqrt{k^2+k_x^2}+i\sqrt{k^2-k_x^2}}$$
$$\times\left[e^{i\sqrt{k^2-k_x^2}y_s}-e^{-\sqrt{k^2+k_x^2}y_s}\right]$$
$$\times\left[-e^{i\sqrt{k^2-k_x^2}y}+e^{-\sqrt{k^2+k_x^2}y}\right]dk_x \quad (38)$$
$$=\frac{2Ci}{\pi}\int_{-\infty}^{\infty}\frac{\exp(ik_x x)}{\Delta_{cs}}f_{cs}(y)f_{cs}(y_s)dk_x, \quad (39)$$

where Δ_{cs} and $f_{cs}(y)$ are given by

$$\Delta_{cs}=-\{\sqrt{k^2+k_x^2}+i\sqrt{k^2-k_x^2}\}, \quad (40)$$

$$f_{cs}(y)=e^{i\sqrt{k^2-k_x^2}y}-e^{-\sqrt{k^2+k_x^2}y}. \quad (41)$$

The fundamental solution for the clamped edge $G_c(\mathbf{r}|\mathbf{r_s};k)$ is obtained by subtracting $\hat{w}_{cs}(\mathbf{r}|\mathbf{r_s})$ from $G_s(\mathbf{r}|\mathbf{r_s};k)$:

$$G_c(\mathbf{r}|\mathbf{r_s};k)=G_s(\mathbf{r}|\mathbf{r_s};k)-\hat{w}_{cs}(\mathbf{r}|\mathbf{r_s}). \quad (42)$$

The Green's function $G_c(\mathbf{r}|\mathbf{r_s};k)$ given by Eq. (42) is convenient for calculating the bending moment per unit length $M_n(\hat{w})$ along the edge $y=0$, since the simply supported solution $G_s(\mathbf{r}|\mathbf{r_s};k)$ does not contribute and the contribution from correction term $-\hat{w}_{cs}(\mathbf{r}|\mathbf{r_s})$ alone needs to be calculated. Along the edge, $M_n(\hat{w})$ is given by

$$M_n(\hat{w})|_{y=0}=\frac{-1}{2\pi}\int_{-\infty}^{\infty}\frac{\exp(ik_x x)}{\sqrt{k^2+k_x^2}+i\sqrt{k^2-k_x^2}}\times[e^{i\sqrt{k^2-k_x^2}y_s}-e^{-\sqrt{k^2+k_x^2}y_s}]dk_x. \quad (43)$$

From Eqs. (33), (19), (22), and (42), we have

$$G_c(\mathbf{r}|\mathbf{r_s};k)=G_\infty(\mathbf{r}|\mathbf{r_s};k)-\tfrac{1}{2}[\hat{w}_{cr}(\mathbf{r}|\mathbf{r_s})+\hat{w}_{cs}(\mathbf{r}|\mathbf{r_s})]. \quad (44)$$

For a clamped edge, both displacement and normal slope must vanish on the boundary. In the derivation from the Green's function of a simply supported edge, the displacement on the boundary is already zero and we need to subtract only the contribution from the normal slope excitation on the boundary to get $G_c(\mathbf{r}|\mathbf{r_s};k)$. Conversely, in the derivation from the roller supported edge, the normal slope along the edge being zero only the contribution from the displacement excitation is subtracted to get $G_c(\mathbf{r}|\mathbf{r_s};k)$. In Eq. (44), we have the free space Green's function $G_\infty(\mathbf{r}|\mathbf{r_s};k)$ which will yield nonzero displacement and normal slope along the line $y=0$. Hence subtract the contributions from both the boundary excitations to arrive at $G_c(\mathbf{r}|\mathbf{r_s};k)$. The multiplicative factor 1/2 in Eq. (44) comes from the fact that the boundary excitations are half that of simply supported and roller boundary conditions. (The choice of image source annuls the two required conditions while doubling the other two.)

D. Free edge via correction to roller supported edge

The Green's function for a free edge $G_f(\mathbf{r}|\mathbf{r_s};k)$ is obtained by modifying $G_r(\mathbf{r}|\mathbf{r_s};k)$ as given by Eq. (22). The simpler problem whose solution is used to construct $G_f(\mathbf{r}|\mathbf{r_s};k)$ is that of a semi-infinite plate with a boundary moment excitation: $M_n=M(k_x)\exp(ik_x x)$ and $V_n=0$ on $y=0$. Using the trial solution given by Eq. (25) and applying the boundary conditions leads to the following system of equations for the coefficients $A(k_x)$ and $B(k_x)$:

$$D\begin{bmatrix} k^2-(1-\nu)k_x^2 & -[k^2+(1-\nu)k_x^2] \\ -i\sqrt{k^2-k_x^2}[k^2+(1-\nu)k_x^2] & -\sqrt{k^2+k_x^2}[k^2-(1-\nu)k_x^2]\end{bmatrix}\times\begin{Bmatrix}A(k_x)\\B(k_x)\end{Bmatrix}=\begin{Bmatrix}M(k_x)\\0\end{Bmatrix}. \quad (45)$$

Solving Eq. (45) gives

$$\hat{w}(\mathbf{r})=\frac{M(k_x)\exp(ik_x x)}{D\Delta}[-\sqrt{k^2+k_x^2}\times\{k^2-(1-\nu)k_x^2\}e^{i\sqrt{k^2-k_x^2}y}+i\sqrt{k^2-k_x^2}\times\{k^2+(1-\nu)k_x^2\}e^{-\sqrt{k^2+k_x^2}y}], \quad (46)$$

where Δ is the determinant of the coefficient matrix given by

$$\Delta=-\sqrt{k^2+k_x^2}\{k^2-(1-\nu)k_x^2\}^2-i\sqrt{k^2-k_x^2}\times\{k^2+(1-\nu)k_x^2\}^2. \quad (47)$$

The coefficient matrix in Eq. (45) is singular when

$$\frac{k_x}{k}=\sqrt[4]{\frac{-(3\nu-1)+2\sqrt{2\nu^2-2\nu+1}}{(1-\nu)^2(3+\nu)}}. \quad (48)$$

For a steel plate with Poisson's ratio $\nu=0.28$, the coefficient matrix is singular when $k_x/k\approx 1.0007$. The null space of the coefficient matrix has dimension 1, which implies that $A(k_x)$ and $B(k_x)$ are nonzero even when there is no boundary excitation. Since we restrict k_x to be on the real (Re) line and k has a small imaginary (Im) part because of the mild dissipation included in the system, the coefficient matrix is never singular, but close to singular when $k_x\approx \mathrm{Re}(k)$.

In a roller supported plate, the component of wave number k_x of the bending moment M_n along the edge is given by Eq. (24) as

$$M(k_x)=\frac{2CD}{\pi}\left[\{k^2-(1-\nu)k_x^2\}\frac{e^{i\sqrt{k^2-k_x^2}y_s}}{\sqrt{k^2-k_x^2}}-i\{k^2+(1-\nu)k_x^2\}\frac{e^{-\sqrt{k^2+k_x^2}y_s}}{\sqrt{k^2+k_x^2}}\right]. \quad (49)$$

The contribution of this bending moment excitation is subtracted from $G_r(\mathbf{r}|\mathbf{r_s};k)$ to realize the free boundary condition along $y=0$. From superposition, the correction to the roller supported fundamental solution $G_r(\mathbf{r}|\mathbf{r_s};k)$ to obtain the solution to the free boundary $G_f(\mathbf{r}|\mathbf{r_s};k)$ is

$$\hat{w}_{fr}(\mathbf{r}|\mathbf{r_s})=\frac{2C}{\pi}\int_{-\infty}^{\infty}\frac{\exp(ik_x x)}{\Delta}\left[\{k^2-(1-\nu)k_x^2\}\times\frac{e^{i\sqrt{k^2-k_x^2}y_s}}{\sqrt{k^2-k_x^2}}-i\{k^2+(1-\nu)k_x^2\}\times\frac{e^{-\sqrt{k^2+k_x^2}y_s}}{\sqrt{k^2+k_x^2}}\right][-\sqrt{k^2+k_x^2}\times\{k^2-(1-\nu)k_x^2\}e^{i\sqrt{k^2-k_x^2}y}+i\sqrt{k^2-k_x^2}\times\{k^2+(1-\nu)k_x^2\}e^{-\sqrt{k^2+k_x^2}y}]dk_x \quad (50)$$

$$=\frac{2C}{\pi}\int_{-\infty}^{\infty}\frac{\exp(ik_x x)}{\Delta_{fr}}f_{fr}(y)f_{fr}(y_s)dk_x, \quad (51)$$

where $f_{fr}(y)$ and Δ_{fr} are given by

$$f_{fr}(y)=-\sqrt{k^2+k_x^2}\{k^2-(1-\nu)k_x^2\}e^{i\sqrt{k^2-k_x^2}y}+i\sqrt{k^2-k_x^2}\{k^2+(1-\nu)k_x^2\}e^{-\sqrt{k^2+k_x^2}y}, \quad (52)$$

$$\Delta_{fr}=-\Delta\sqrt{k^2+k_x^2}\sqrt{k^2-k_x^2}. \quad (53)$$

The Green's function for the free edge $G_f(\mathbf{r}|\mathbf{r_s};k)$ is obtained by subtracting $\hat{w}_{fr}(\mathbf{r}|\mathbf{r_s})$ from $G_r(\mathbf{r}|\mathbf{r_s};k)$.

$$G_f(\mathbf{r}|\mathbf{r_s};k)=G_r(\mathbf{r}|\mathbf{r_s};k)-\hat{w}_{fr}(\mathbf{r}|\mathbf{r_s}). \quad (54)$$

E. Free edge via correction to simply supported edge

In this section, the Green's function for a free edge $G_f(\mathbf{r}|\mathbf{r_s};k)$ is obtained by modifying $G_s(\mathbf{r}|\mathbf{r_s};k)$ given by Eq.

(19). The simpler problem whose solution is used to construct $G_f(\mathbf{r}|\mathbf{r_s};k)$ is that of a semi-infinite plate with a boundary force excitation: $M_n=0$ on $y=0$ and $V_n=V(k_x)\times\exp(ik_x x)$ on $y=0$. Using the trial solution given by Eq. (25) and applying the boundary conditions leads to the following system of equations for the coefficients $A(k_x)$ and $B(k_x)$:

$$D\begin{bmatrix} k^2-(1-\nu)k_x^2 & -[k^2+(1-\nu)k_x^2] \\ -i\sqrt{k^2-k_x^2}[k^2+(1-\nu)k_x^2] & -\sqrt{k^2+k_x^2}[k^2-(1-\nu)k_x^2] \end{bmatrix} \times \begin{Bmatrix} A(k_x) \\ B(k_x) \end{Bmatrix} = \begin{Bmatrix} 0 \\ V(k_x) \end{Bmatrix}. \tag{55}$$

Solving Eq. (55) gives

$$\hat{w}(\mathbf{r})=\frac{V(k_x)\exp(ik_x x)}{D\Delta}[\{k^2+(1-\nu)k_x^2\}e^{i\sqrt{k^2-k_x^2}y}+\{k^2-(1-\nu)k_x^2\}e^{-\sqrt{k^2+k_x^2}y}], \tag{56}$$

where Δ is the determinant of the coefficient matrix given by Eq. (47). In a simply supported plate, the component of wave number k_x of the edge reaction V_n along the edge is given by Eq. (21) as

$$V(k_x)=\frac{2CDi}{\pi}[\{k^2+(1-\nu)k_x^2\}e^{i\sqrt{k^2-k_x^2}y_s}+\{k^2-(1-\nu)k_x^2\}e^{-\sqrt{k^2+k_x^2}y_s}]. \tag{57}$$

The contribution of this force excitation is subtracted from $G_s(\mathbf{r}|\mathbf{r_s};k)$ to realize the free boundary condition along $y=0$. From superposition, the correction to the simply supported fundamental solution $G_s(\mathbf{r}|\mathbf{r_s};k)$ to obtain the solution to the free boundary $G_f(\mathbf{r}|\mathbf{r_s};k)$ is

$$\begin{aligned}\hat{w}_{fs}(\mathbf{r}|\mathbf{r_s})&=\frac{2Ci}{\pi}\int_{-\infty}^{\infty}\frac{\exp(ik_x x)}{\Delta}[\{k^2+(1-\nu)k_x^2\}\\&\quad\times e^{i\sqrt{k^2-k_x^2}y_s}+\{k^2-(1-\nu)k_x^2\}e^{-\sqrt{k^2+k_x^2}y_s}]\\&\quad\times[\{k^2+(1-\nu)k_x^2\}e^{i\sqrt{k^2-k_x^2}y}\\&\quad+\{k^2-(1-\nu)k_x^2\}e^{-\sqrt{k^2+k_x^2}y}]dk_x \qquad (58)\\&=\frac{2Ci}{\pi}\int_{-\infty}^{\infty}\frac{\exp(ik_x x)}{\Delta_{fs}}f_{fs}(y)f_{fs}(y_s)dk_x, \qquad (59)\end{aligned}$$

where $\Delta_{fs}=\Delta$ and $f_{fs}(y)$ is given by

$$f_{fs}(y)=\{k^2+(1-\nu)k_x^2\}e^{i\sqrt{k^2-k_x^2}y}+\{k^2-(1-\nu)k_x^2\}e^{-\sqrt{k^2+k_x^2}y}. \tag{60}$$

The Green's function for the free edge $G_f(\mathbf{r}|\mathbf{r_s};k)$ is obtained by subtracting $\hat{w}_{fs}(\mathbf{r}|\mathbf{r_s})$ from $G_s(\mathbf{r}|\mathbf{r_s};k)$:

$$G_f(\mathbf{r}|\mathbf{r_s};k)=G_s(\mathbf{r}|\mathbf{r_s};k)-\hat{w}_{fs}(\mathbf{r}|\mathbf{r_s}). \tag{61}$$

From Eqs. (54) and (61) we obtain the following relation which is similar to the clamped boundary condition solution:

$$G_c(\mathbf{r}|\mathbf{r_s};k)=G_\infty(\mathbf{r}|\mathbf{r_s};k)-\tfrac{1}{2}[\hat{w}_{fr}(\mathbf{r}|\mathbf{r_s})+\hat{w}_{fs}(\mathbf{r}|\mathbf{r_s})]. \tag{62}$$

III. CLENSHAW–CURTIS INTEGRATION OF WAVE-NUMBER INTEGRALS OVER FINITE INTERVALS

The wave-number integrals occurring in the expressions for the Green's functions of a semi-infinite plate are in the form of improper (infinite) integrals as given by Eqs. (29), (38), (50), and (58). For the purpose of numerical quadrature, these are broken down into many finite integrals. These integrals typically are of the form $\int_a^b g(x,k_x)\cos(k_x x)dk_x$ and $\int_a^b g(x,k_x)\sin(k_x x)dk_x$. Filon[13] developed a method in which integrals of this type are approximately evaluated by fitting a quadratic polynomial to the function $g(x,k_x)$ over each subinterval and integrating each term analytically. This method is accurate when $g(x,k_x)$ is slowly varying. In the case of integrals occurring in the Green's function expressions, $g(x,k_x)$ is often irregular, and sometimes almost singular. Clenshaw and Curtis[14] developed a powerful method that can handle these irregularities. The function $g(x,k_x)$ is approximated by a finite series of Chebyshev polynomials of the first kind $T_m(z)$, followed by an analytical integration of each term in the series. Xu and Mal[15] derived an error estimate for the eighth order formula using the Clenshaw and Curtis method. Dravinski and Mossessian[16] demonstrated the use of Xu and Mal's approach in calculating the Green's functions for harmonic line loads in a viscoelastic half-space.

A brief outline of this method, commonly referred to as the Clenshaw–Curtis integration, is given next. Define, for later use, the functions $I_m(t)$ and $J_m(t)$ along with their recursive expressions as follows:

$$I_m(t)=\int_{-1}^{1}T_m(z)e^{itz}dz, \tag{63}$$

$$\begin{aligned}I_0(t)&=\frac{-i}{t}(e^{it}-e^{-it}),\\I_1(t)&=\frac{e^{it}+e^{-it}}{it}+\frac{1}{t^2}(e^{it}-e^{-it}),\\I_2(t)&=\left(\frac{4i}{t}\right)I_1(t)-\frac{i}{t}(e^{it}-e^{-it}),\\I_{m+1}(t)&=\frac{2i(m+1)}{t}I_m(t)+\frac{m+1}{m-1}I_{m-1}(t)\\&\quad+\frac{2i}{t(m-1)}(e^{it}+(-1)^m e^{-it})\quad\text{for } m\geqslant 2,\end{aligned} \tag{64}$$

$$J_m(t)=\int_{-1}^{1}T_m(z)e^{-itz}dz, \tag{65}$$

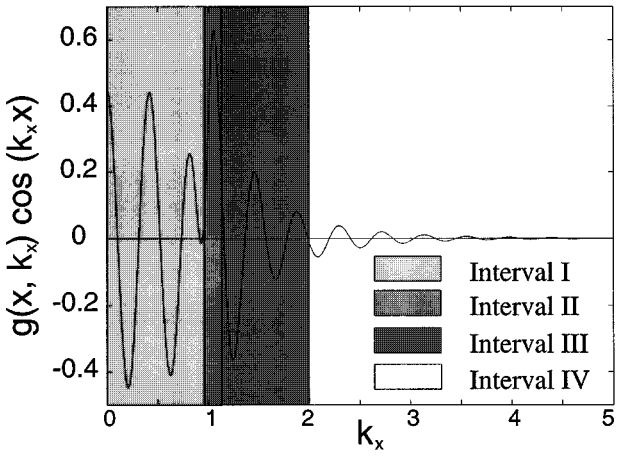

FIG. 2. A typical wave-number integrand with a near singularity at $k_x=1.0$.

$$
\begin{aligned}
J_0(t)&=\frac{i}{t}(e^{-it}-e^{it}),\\
J_1(t)&=\frac{e^{-it}+e^{it}}{(-i)t}+\frac{1}{t^2}(e^{-it}-e^{it}),\\
J_2(t)&=\frac{-4i}{t}J_1(t)+\frac{i}{t}(e^{-it}-e^{it}),\\
J_{m+1}(t)&=\frac{-2i}{t}(m+1)J_m(t)+\frac{(m+1)}{(m-1)}J_{m-1}(t)\\
&\quad+\frac{(-2i)}{t(m-1)}(e^{-it}+(-1)^m e^{it}) \quad \text{for } m\geqslant 2.
\end{aligned}
\tag{66}
$$

Define $G_{m,j}$ and its recursive relations as

$$
G_{m,j}=-\int_{-1}^{1}T_m(z)z^j dz, \tag{67}
$$

$$
\begin{aligned}
G_{0,j}&=\frac{1+(-1)^j}{j+1},\\
G_{1,j}&=G_{0,j+1},\\
G_{m,j}&=2G_{m-1,j+1}-G_{m-2,j} \quad \text{for } m\geqslant 2.
\end{aligned}
\tag{68}
$$

Given a function $g(x,k_x)$ that has to be integrated over the interval $k_x\in[a,b]$, first normalize the range of integration to $[-1,1]$ by introducing the function $k_x=Az+B$, where $A=(b-a)/2$, $B=(b+a)/2$. This function is approximated by a finite Chebyshev series as follows:

$$
g(x,k_x)=g(x,Az+B)=f(x,z)\approx\sum_{m=0}^{N}{}''\,D_m(x)T_m(z). \tag{69}
$$

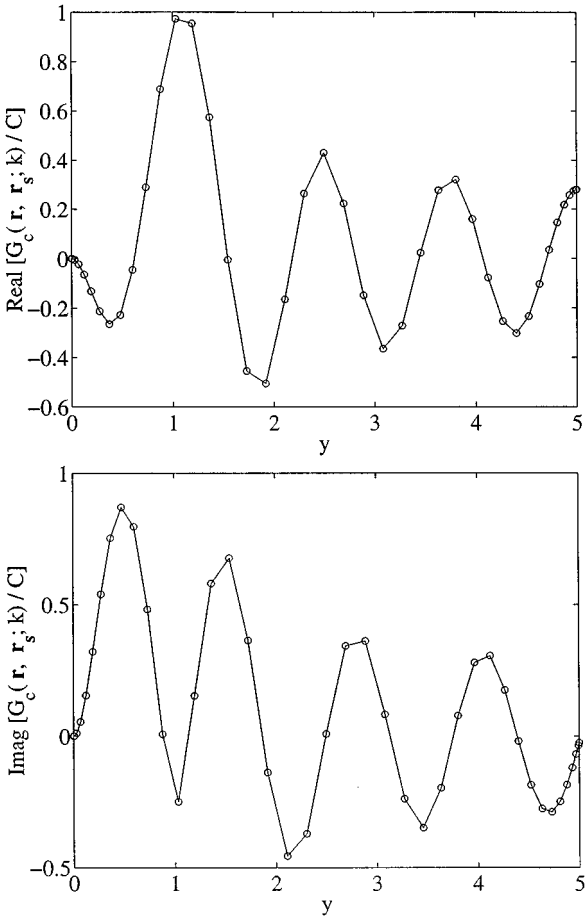

FIG. 3. Comparison of the $G_c(\mathbf{r},\mathbf{r}_s;k)$ given by Eqs. (33) and (44) along $x=0$ for a semi-infinite plate with a clamped edge. Key: ———, Eq. (33); ○, Eq. (44).

The unknown constants $D_m(x)$ are calculated using

$$
D_m(x)=\frac{2}{N}\sum_{j=0}^{N}{}''\,f\left(x,\cos\left(\frac{j\pi}{N}\right)\right)\cos\left(\frac{mj\pi}{N}\right). \tag{70}
$$

The double prime on the summation symbol denotes summation over a sequence whose first and last terms are halved:

$$
\sum_{m=0}^{N}{}''\,s_m=\frac{s_0}{2}+s_1+s_2+\cdots+s_{N-1}+\frac{s_N}{2}. \tag{71}
$$

The Clenshaw–Curtis quadrature formula is expressed in terms of these functions as follows:

TABLE I. Numerical evaluation of the Hankel function H_0^1 using wave-number integral.

θ	$\mathrm{Re}[H_0^1(\exp(i\theta))]$	$\mathrm{Im}[H_0^1(\exp(i\theta))]$	NS	Error
1	0.751 678 646 346 771 8	8.059 102 803 424 181 3E-02	714	0.1234E-11
30	0.438 513 077 962 303 7	−0.112 818 452 396 018 9	265	0.2121E-10
60	0.204 526 564 082 411 5	−0.230 704 377 271 396 3	204	0.3614E-10
90	0.000 000 000 000 000 0	−0.268 032 482 033 987 1	170	0.4815E-10

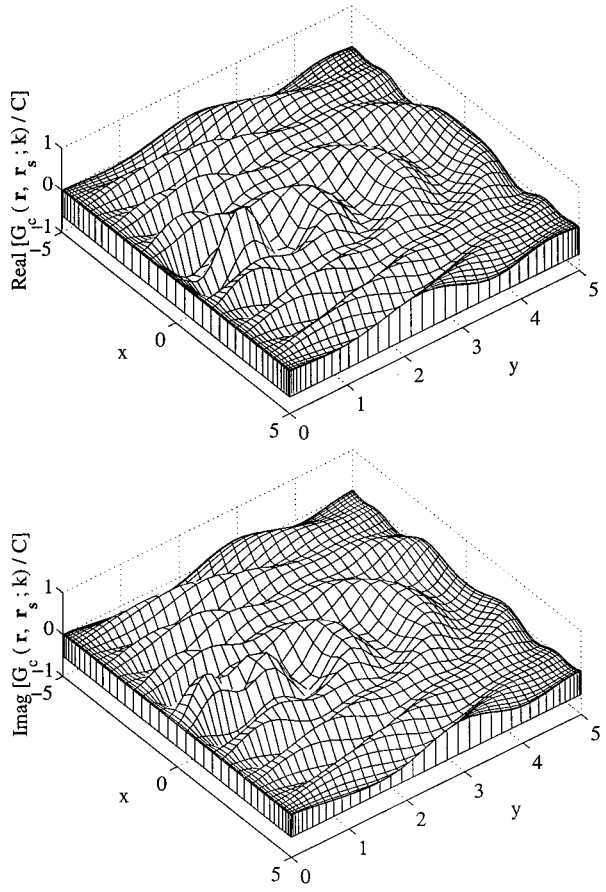

FIG. 4. Vibratory response $G_c(\mathbf{r},\mathbf{r}_s;k)$ for $(x,y)\in[-5,+5]\times[0,5]$ for a semi-infinite plate with a clamped edge.

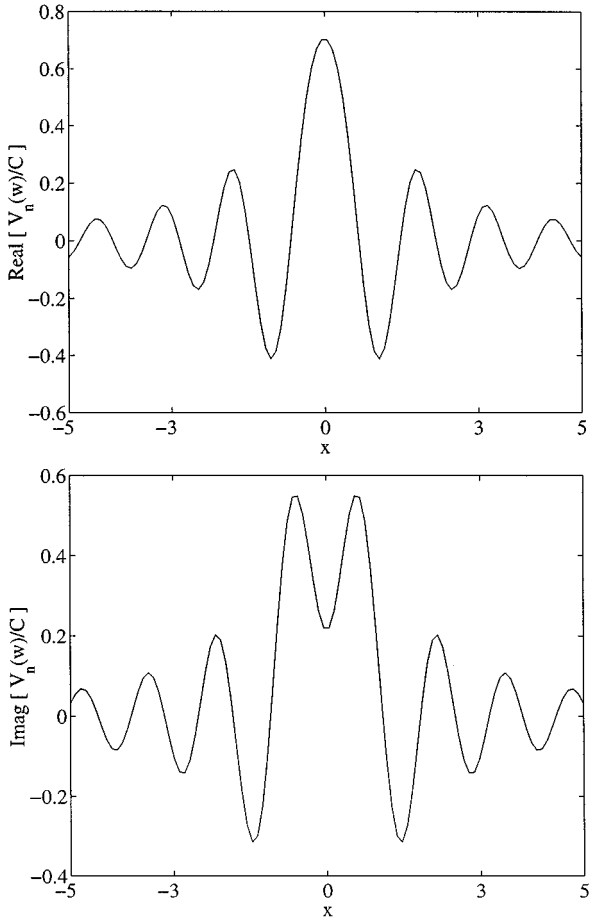

FIG. 5. Effective shear force distribution $V_n(\hat{w})$ along the x axis for a semi-infinite plate with a clamped edge.

$$\int_a^b g(x,k_x)e^{ik_x x}dk_x$$

$$=\begin{cases} Ae^{ixB}\sum_{m=0}^{N}{}'' D_m(x)I_m(Ax) & \text{for } |Ax|>1 \\ Ae^{ixB}\sum_{m=0}^{N}{}'' D_m(x)\sum_{j=0}^{\infty} G_{m,j}\dfrac{(iAx)^j}{j!} & \text{for } |Ax|\leqslant 1, \end{cases} \tag{72}$$

$$\int_a^b g(x,k_x)e^{-ik_x x}dk_x$$

$$=\begin{cases} Ae^{-ixB}\sum_{m=0}^{N}{}'' D_m(x)J_m(Ax) & \text{for } |Ax|>1 \\ Ae^{-ixB}\sum_{m=0}^{N}{}'' D_m(x)\sum_{j=0}^{\infty} G_{m,j}\dfrac{(-iAx)^j}{j!} & \text{for } |Ax|\leqslant 1. \end{cases} \tag{73}$$

When $N=8$, the error in these quadrature formulas is estimated by Xu and Mal[15] as

$$\epsilon=\max(2.5|D_8(x)|,2.0|D_7(x)|,1.5|D_6(x)|,1.2|D_5(x)|). \tag{74}$$

Using the definitions of the trigonometric functions in terms of the exponential functions,

$$\int_a^b g(x,k_x)\cos(k_x x)dk_x=\frac{1}{2}\left(\int_a^b g(x,k_x)e^{ik_x x}dk_x + \int_a^b g(x,k_x)e^{-ik_x x}dk_x\right), \tag{75}$$

$$\int_a^b g(x,k_x)\sin(k_x x)dk_x=\frac{1}{2i}\left(\int_a^b g(x,k_x)e^{ik_x x}dk_x - \int_a^b g(x,k_x)e^{-ik_x x}dk_x\right). \tag{76}$$

If the error estimate ϵ for numerically evaluated integrals is larger than a prescribed tolerance value, then the interval is subdivided into two halves, and the process is repeated for each of the subintervals. The interval subdivision is repeated until the error estimate becomes smaller than the tolerance value. Hence this method is designated as ''adaptive integration.'' More subdivisions are required when the function has a near singularity in the interval of integration.

IV. EVALUATION OF IMPROPER WAVE-NUMBER INTEGRALS OCCURRING IN GREEN'S FUNCTION FORMULAS

The previous section showed how to evaluate wave-number integrals over a finite interval. Green's function ex-

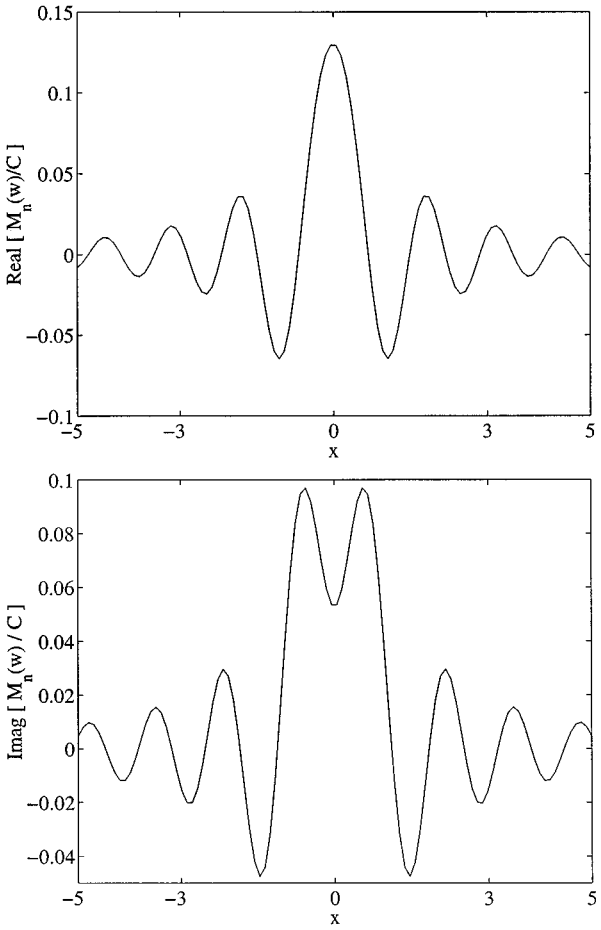

FIG. 6. Bending moment distribution $M_n(\hat{w})$ along the x axis for a semi-infinite plate with a clamped edge.

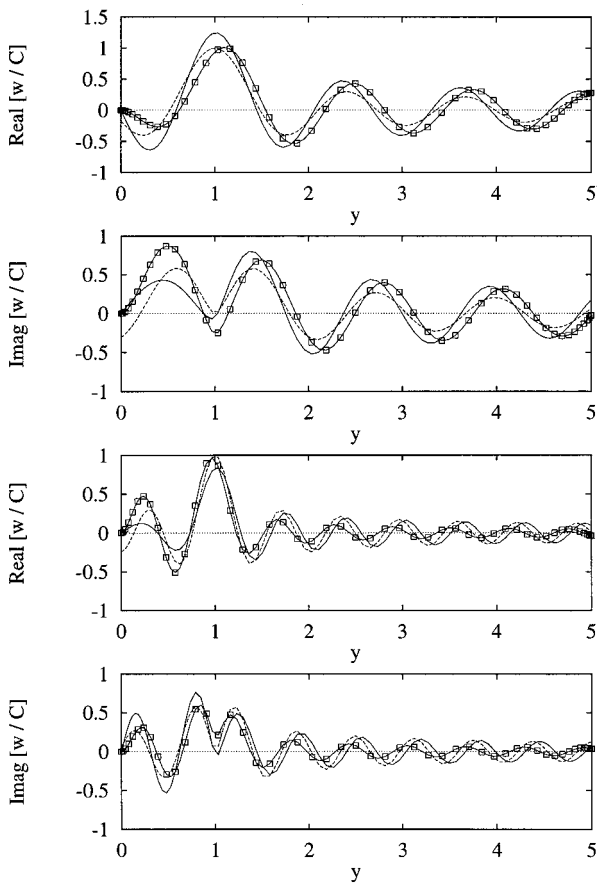

FIG. 7. Comparison of $G_c(\mathbf{r},\mathbf{r_s};k)$ with $G_s(\mathbf{r},\mathbf{r_s};k)$ for $y_s=1$, $k=5+0.005i$ (top two), and $k=10+0.01i$ (bottom two) along the y-axis for a semi-infinite plate with clamped and simply supported edges respectively. Key: —□—, $G_c(\mathbf{r},\mathbf{r_s};k)$; ———, $G_s(\mathbf{r},\mathbf{r_s};k)$; dashed line, $G_\infty(\mathbf{r},\mathbf{r_s};k)$.

pressions contain improper wave-number integrals of the form $\int_0^\infty g(x,k_x)\cos(k_x x)dk_x$ and $\int_0^\infty g(x,k_x)\sin(k_x x)dk_x$. This section shows how these improper integrals are expressed as a series of finite integrals, and how the sum of the resulting series is calculated. The integrands in these improper integrals oscillate rapidly. The function $g(x,k_x)$ can have very sharp peaks at the particular values of k_x corresponding to the real part of a pole. Also, the functions $g(x,k_x)$ attenuate very slowly resulting in poor convergence. Because of these two reasons, conventional numerical integration methods are not satisfactory.

Figure 2 shows the behavior typical of such wave-number integrals. Let I be the wave-number integral of interest.

$$I=\int_0^\infty g(x,k_x)\cos(k_x x)dk_x, \tag{77}$$

where $k_x=s_0$ is the location of the peak in the integrand. Let s_1 be a multiple of π/x large enough that the irregularities at $k_x=s_0$ have died down before $k_x=s_1$. Here, s_1 is chosen such that the function $g(x,k_x)$ has no poles or zeroes when $k_x>s_1$. The integral I is divided into four parts as shown in Fig. 2:

$$I=I_1+I_{\rm II}+I_{\rm III}+I_{\rm IV}, \tag{78}$$

$$\begin{aligned}
I_1&=\int_0^{s_0-\varepsilon} g(x,k_x)\cos(k_x x)dk_x,\\
I_{\rm II}&=\int_{s_0-\varepsilon}^{s_0+\varepsilon} g(x,k_x)\cos(k_x x)dk_x,\\
I_{\rm III}&=\int_{s_0+\varepsilon}^{s_1} g(x,k_x)\cos(k_x x)dk_x,\\
I_{\rm IV}&=\int_{s1}^{\infty} g(x,k_x)\cos(k_x x)dk_x.
\end{aligned} \tag{79}$$

The first three integrals are evaluated using the adaptive Clenshaw–Curtis quadrature method that was described in Sec. III. The integral $I_{\rm II}$ is further subdivided into two equal subintervals before quadrature if the near singularity at $k_x=s_0$ is very strong. The last part, $I_{\rm IV}$ is an improper integral with the near singularity removed. The integral $I_{\rm IV}$ can be expressed as

$$I_{\rm IV}=\int_{s1}^{\infty} g(x,k_x)\cos(k_x x)dk_x=\int_{s_1}^{s_2}(\cdots)+\int_{s_2}^{s_3}(\cdots)+\int_{s_3}^{s_4}(\cdots)+\cdots, \tag{80}$$

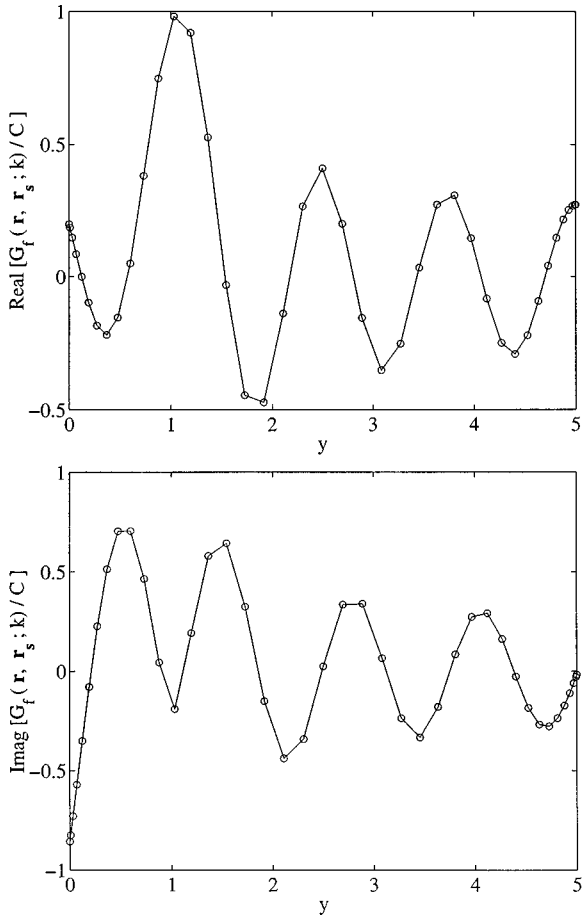

FIG. 8. Comparison of the $G_f(\mathbf{r},\mathbf{r}_s;k)$ given by Eqs. (54) and (61) along $x=0$ for a semi-infinite plate with a free edge. Key: ———, Eq. (54); ○, Eq. (61).

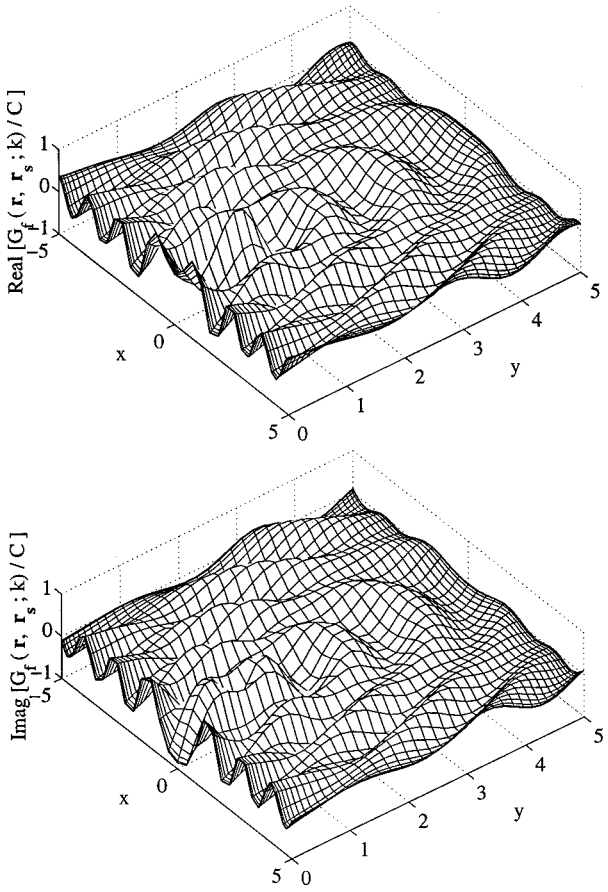

FIG. 9. Vibratory response $G_f(\mathbf{r},\mathbf{r}_s;k)$ for $(x,y)\in[-5,+5]\times[0,5]$ for a semi-infinite plate with a free edge.

where $s_2,s_3,s_4,\ldots$ are the consecutive integer multiples of π/x. This infinite series of subintegrals is an alternating series, with each term being opposite in sign to its preceding term. Therefore I_{IV} can be expressed as

$$I_{\mathrm{IV}}=A_1-A_2+A_3-A_4+A_5-\cdots . \tag{81}$$

All of the terms $A_1,A_2,A_3,A_4,A_5,\ldots$ have the same sign and each can be evaluated by the adaptive Clenshaw–Curtis method. The absolute series is monotonously decreasing. Longman[17] described a method in which slowly converging alternating series of this kind can be transformed into swiftly converging series. According to Euler's transformation define the forward difference terms:

$$\begin{aligned}&\Delta A_m=A_{m+1}-A_m,\\ &\Delta^{r+1}A_m=\Delta^r A_{m+1}-\Delta^r A_m .\end{aligned} \tag{82}$$

Then the series after transformation is

$$\sum_{m=0}^{\infty}(-1)^m A_m=\frac{1}{2}A_0-\frac{1}{4}\Delta A_0+\frac{1}{8}\Delta^2 A_0-\frac{1}{16}\Delta^3 A_0+\cdots . \tag{83}$$

The remainder R_p after p terms is bounded by $2^{-p}|\Delta^p A_0|$. Thus the slowly converging series has been converted to a rapidly converging series. This series summation is carried out with as many terms as are needed to make this error smaller than the tolerance value. Shank's paper[18] contains an extensive treatment of Euler's transformation and other nonlinear sequence-to-sequence transformations. The effectiveness of these transforms in accelerating convergence in some slowly converging series and in inducing convergence in some diverging series is discussed. Difficulties which sometimes arise in the use of these transforms such as nonuniform convergence to the wrong answer, irregularity and the ambiguity of multivalued functions are also investigated. Dravinski and Mossessian[16] have also successfully used Euler's transformation to evaluate wave-number integrals.

To demonstrate the accuracy of the adaptive integration technique described in the Sec. III, the zero order Hankel function of the first kind given in the wave-number integral form by Eq. (17) is compared with the conventional series summation form. The symbolic computational program MAPLE[19] is used to calculate the Hankel function accurately to 20 decimal places and it is taken as the exact value with which the wave-number integral is compared. Figure 2 shows the real part of the integrand. The integral is evaluated in double precision with the tolerance set at $\epsilon=1.0\mathrm{E}-11$. In Table I, NS is the number of subintervals required, which is a measure of the number of function evaluations needed, and the error is the absolute distance between the exact and calculated values. From the results of Table I, it is clear that the adaptive integration technique is very accurate.

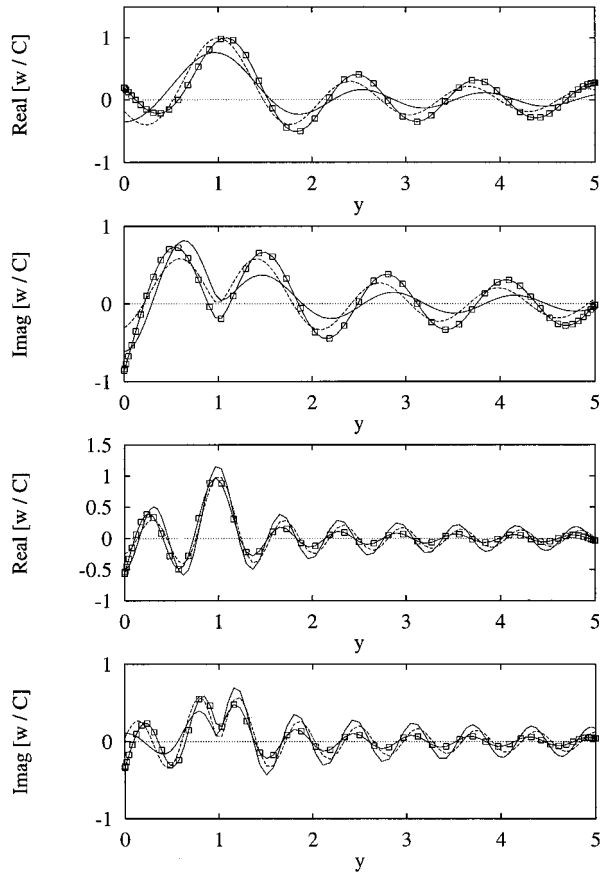

FIG. 10. Comparison of $G_f(\mathbf{r},\mathbf{r_s};k)$ with $G_r(\mathbf{r},\mathbf{r_s};k)$ for $y_s=1$, $k=5+0.005i$ (top two) and $k=10+0.01i$ (bottom two) along the y-axis for a semi-infinite plate with free and roller supported edges, respectively. Key: —□—, $G_f(\mathbf{r},\mathbf{r_s};k)$; ———, $G_r(\mathbf{r},\mathbf{r_s};k)$; dashed line, $G_\infty(\mathbf{r},\mathbf{r_s};k)$.

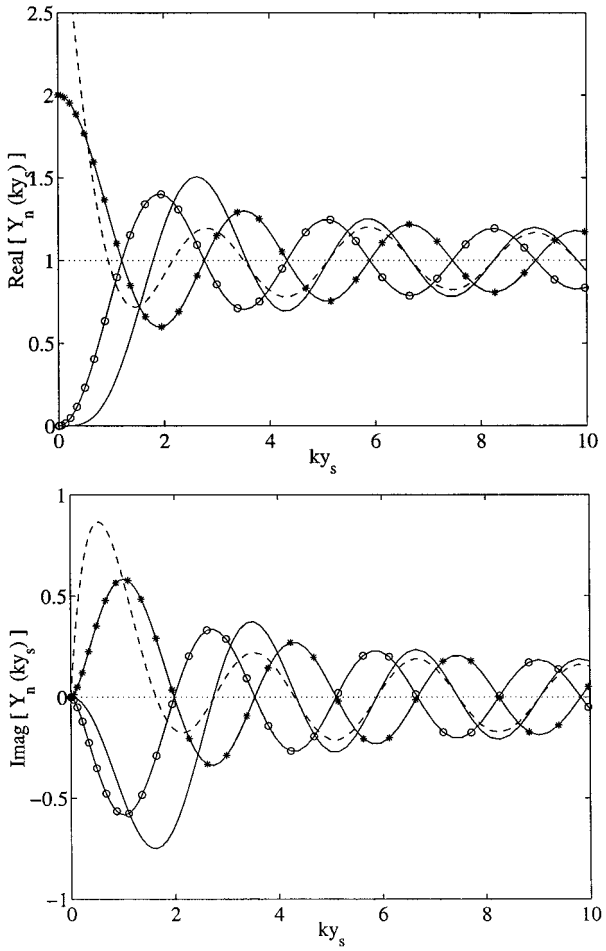

FIG. 11. Normalized driving point mobility $\hat{Y}_n(ky)$ for a semi-infinite plate with different edge conditions. Key: ———, clamped edge; ----, free edge; —○—, simply supported edge; —*—, roller supported edge. Note that $\mathrm{Re}(\hat{Y}_n)=1$, $\mathrm{Im}(\hat{Y}_n)=0$ correspond to the driving point mobility of an infinite plate.

V. RESULTS AND DISCUSSION

For the sake of illustration, the excitation point is located at $(x_s,y_s)=(0,1)$ and a bending wave number of $k=5+0.005i$ is chosen for a semi-infinite plate with a clamped edge. The observation location in the semi-infinite plate is restricted to $(x,y)\in[-5,+5]\times[0,5]$. The two representations for the Green's function $G_c(\mathbf{r},\mathbf{r_s};k)$ given by Eqs. (33) and (42) are compared in Fig. 3 from which it can be inferred that both solutions are practically identical. The calculation using Eq. (42) is faster because its integrand does not have a near singularity in the interval of integration. The vibratory response is depicted in Fig. 4. The shear force and bending moment distributions along the plate edge $(y=0)$ are plotted in Figs. 5 and 6, respectively. The solutions with clamped and simply supported boundary conditions $G_c(\mathbf{r},\mathbf{r_s};k)$ and $G_s(\mathbf{r},\mathbf{r_s};k)$ are compared in Fig. 7 to study the influence of the clamping term as the excitation frequency increases. As expected, from Fig. 7 it is seen that the solutions behave quite differently near the edge $y=0$, but in the vicinity of the source $(y_s=1)$ the infinite plate Green's function $G_\infty(\mathbf{r},\mathbf{r_s};k)$ dominates the response. Away from the source and the edge, all the solutions fall off because of geometric spreading that is given by the $1/\sqrt{r}$ term.

Similarly, for the numerical study of a plate with a free edge, we choose the same excitation location $(x_s,y_s)=(0,1)$, bending wave number of $k=5+0.005i$, and the observation domain $(x,y)\in[-5,+5]\times[0,5]$, as in the clamped case. The two representations for the Green's function $G_f(\mathbf{r},\mathbf{r_s};k)$ given by Eqs. (54) and (61) are compared in Fig. 8 and found to be identical. The vibratory response is shown in Fig. 9. The solutions with free and roller supported boundary conditions $G_f(\mathbf{r},\mathbf{r_s};k)$ and $G_r(\mathbf{r},\mathbf{r_s};k)$ are compared in Fig. 10 from which the edge and source effects are apparent.

It should be noted that Eqs. (30), (39), (51), and (59) are all symmetric with respect to $\mathbf{r}$ and $\mathbf{r_s}$, since the solution should remain unchanged when the source and the observation locations are interchanged, because of reciprocity. It is well known that the driving point mobility of a infinite plate $\hat{Y}_\infty(k)$ is real valued and independent of excitation frequency. This result can be directly obtained from $G_\infty(\mathbf{r},\mathbf{r_s};k)$ as

$$\hat{Y}_\infty(k)=\lim_{\mathbf{r}\to\mathbf{r_s}} -i\omega G_\infty(\mathbf{r},\mathbf{r_s};k)=-i\omega C=\frac{1}{8\sqrt{\rho hD}}. \quad (84)$$

In Fig. 11, the normalized driving point mobilities $\hat{Y}_n(ky_s)=\hat{Y}(ky_s)/\hat{Y}_\infty$ are plotted. For all of the classical boundary conditions considered in this article, the mobility

curves approach that of a infinite plate asymptotically as $ky_s \gg 1$.

VI. CONCLUSION

New analytical harmonic Green's functions for a semi-infinite plate with clamped or free edges are developed. Two solutions are derived for each boundary condition starting from either roller or simply supported solutions. The formal solutions in terms of improper wave-number integrals are numerically evaluated using eighth order Clenshaw–Curtis adaptive quadrature. The procedure developed in this paper may be extended further to derive the Green's functions of semi-infinite plates with impedance type boundary conditions. These Green's functions will be of use to researchers interested in developing boundary element models for semi-infinite plates with arbitrary holes or cutouts, and to us in our continuing effort to build a ray tracing model for finite polygonal plates.

ACKNOWLEDGMENTS

This work has been supported by the U.S. Army Research Office (URI Grant No. DAAL-03-92-G-0120; Project Monitor: Dr. T. L. Doligalski).

[1] R. Gunda, S. M. Vijayakar, and R. Singh, ''Method of images for the harmonic response of beams and rectangular plates,'' J. Sound Vib. **185**, 791 (1995).
[2] H. Lamb, ''On the propagation of tremors over the surface of an elastic solid,'' Philos. Trans. R. Soc. London, Ser. A **203**, 1–42 (1904).
[3] E. R. Lapwood, ''The disturbance due to a line source in a semi-infinite elastic medium,'' Philos. Trans. R. Soc. London, Ser. A **242**, 63–100 (1949).
[4] A. N. Jette and J. G. Parker, ''Excitation of an elastic half-space by a buried line source of conical waves,'' J. Sound Vib. **67**, 523–531 (1979).
[5] D. M. Photiadis, ''Approximations for the two-dimensional Green's function of a fluid-loaded plate,'' J. Acoust. Soc. Am. **93**, 42–47 (1993).
[6] J. M. Cushchieri and D. Feit, ''A hybrid numerical and analytical solution for the Green's function of a fluid loaded elastic plate,'' J. Acoust. Soc. Am. **95**, 1998–2005 (1994).
[7] N. Ortner and P. Wagner, ''The Green's functions of clamped semi-infinite vibrating beams and plates,'' Int. J. Solids Struct. **26**, 237–249 (1990).
[8] A. D. Kerr, ''The clamped semi-infinite plate on a winkler base subjected to a vertical force,'' Q. J. Mech. Appl. Math. **46**, 457–470 (1993).
[9] A. W. Leissa, *Vibration of Plates* (Acoustical Society of America, Woodbury, NY, 1993), 2nd ed.
[10] Y. Niwa, S. Kobayashi, and M. Kitahara, ''Eigen frequency analysis of a plate by the integral equation method,'' Theor. Appl. Mech. **29**, 287–367 (1981).
[11] N. N. Lebedev, *Special Functions and their Applications* (Dover, New York, 1972).
[12] K. F. Graff, *Wave Motion in Elastic Solids* (Dover, New York, 1991).
[13] L. N. G. Filon, ''On a quadrature formula for trigonometric integrals,'' Proc. R. Soc. Edinburgh **49**, 38–47 (1928).
[14] C. W. Clenshaw and A. R. Curtis, ''A method for numerical integration on a automatic computer,'' Numer. Math. **2**, 197–205 (1960).
[15] P.-C. Xu and A. K. Mal, ''An adaptive integration scheme for irregularly oscillatory functions,'' Wave Motion **7**, 235–243 (1985).
[16] M. Dravinski and T. K. Mossessian, ''On the evaluation of Green's functions for harmonic line loads in a viscoelastic halfspace,'' Int. J. Numer. Methods Eng. **26**, 823–841 (1988).
[17] I. M. Longman, ''Note on a method for computing infinite integrals of oscillatory functions,'' Proc. Cambridge Philos. Soc. **52**, 764–768 (1956).
[18] D. Shanks, ''Non-linear transformations of divergent and slowly convergent sequences,'' J. Math. Phys. **34**, 1–42 (1955).
[19] Waterloo Maple Inc. MAPLE *V Release 4, Version 4.00f*, 1996.